AIP | Review of Scientific Instruments

Identification and mitigation of stray laser light in the Thomson scattering system on the Madison Symmetric Torus (MST)

C. M. Jacobson, M. T. Borchardt, D. J. Den Hartog, A. F. Falkowski, L. A. Morton, and M. A. Thomas

Citation: Review of Scientific Instruments **87**, 11E511 (2016); doi: 10.1063/1.4960063
View online: http://dx.doi.org/10.1063/1.4960063
View Table of Contents: http://scitation.aip.org/content/aip/journal/rsi/87/11?ver=pdfcov
Published by the AIP Publishing

REVIEW OF SCIENTIFIC INSTRUMENTS **87**, 11E511 (2016)

Identification and mitigation of stray laser light in the Thomson scattering system on the Madison Symmetric Torus (MST)

C. M. Jacobson,[a)] M. T. Borchardt, D. J. Den Hartog, A. F. Falkowski,[b)] L. A. Morton, and M. A. Thomas
Department of Physics, University of Wisconsin–Madison, 1150 University Avenue, Madison, Wisconsin 53706, USA

(Presented 8 June 2016; received 5 June 2016; accepted 6 July 2016; published online 1 August 2016)

The Thomson scattering diagnostic on the Madison Symmetric Torus (MST) records excessive levels of stray Nd:YAG laser light. Stray light saturates the 1064 nm spectral channel in all polychromators, which prevents absolute electron density measurements via Rayleigh scattering calibration. Furthermore, stray light contaminates adjacent spectral channels for $r/a \geq 0.75$, which renders the diagnostic unable to make electron temperature measurements at these radii. *In situ* measurements of stray light levels during a vacuum vessel vent are used to identify stray light sources and strategies for reduction of stray light levels. Numerical modeling using Zemax OpticStudio supports these measurements. The model of the vacuum vessel and diagnostic includes synthetic collection optics to enable direct comparison of measured and simulated stray light levels. Modeling produces qualitatively similar stray light distributions to MST measurements, and quantifies the mitigation effects of stray light mitigation strategies prior to implementation. *Published by AIP Publishing.* [http://dx.doi.org/10.1063/1.4960063]

I. INTRODUCTION

The Thomson scattering diagnostic[1] on the Madison Symmetric Torus[2] (MST) records excessive levels of stray Nd:YAG laser light at 1064 nm. Stray light saturates the 1064 nm spectral channel in all polychromators, which prevents absolute electron density n_e measurements via Rayleigh scattering calibration. Furthermore, stray light contaminates adjacent spectral channels for $r/a \geq 0.75$, which renders the diagnostic unable to make electron temperature T_e measurements at these radii.

Stray light mitigation techniques include the addition of properly sized and positioned apertures,[3,4] spatial filters,[5] well-designed beam dumps,[6] and viewing dumps.[7] A critical aperture can constrain the primary stray light cone, which originates from surface scatter on the last optical element. A larger diameter subcritical aperture can constrain the secondary stray light cone, which is the result of scatter off the critical aperture. For effective reduction of stray light, both cones should be limited to be within the exit port.[3] However, the present configuration of the MST Thomson scattering beam line only allows the primary stray light cone to be contained at the exit port. To limit field error, MST conducting shell porthole sizes are restricted. Since the beam line is vertical, instead of horizontal as is typical in other devices, it is more difficult to extend the flight tube back from the vessel. Installation of a viewing dump would create an undesirable limiting surface for the plasma. Discrimination of Thomson scattered light from stray light using time of flight techniques is not possible as the path length through the vessel is 1.04 m and the beam pulse width is 20 ns. An additional difficulty is that two laser beams on slightly different beam lines pass through the plasma. Due to these challenges, both experimental measurements and numerical modeling are used to identify sources of stray light and test mitigation strategies.

II. EXPERIMENTAL MEASUREMENTS

The MST Thomson scattering[1] beam line is 15 m long and has five turning mirrors, the final of which is 1.66 m above the vessel midplane. The beams are then focused by a $f = 2.03$ m lens located 1.25 m above the midplane such that the beam waist is located approximately at the exit port 0.52 m below the midplane. The beams enter vacuum after passing through a Brewster window, then traverse a flight tube, pass into the plasma volume, then the pump duct, alignment probe box, and flight tube, and finally exit the vacuum at a second Brewster window before impacting the beam dump.

Identification of sources of stray light and tests of mitigation strategies are performed during a vent of the MST vacuum vessel. Stray light levels are measured by firing the Spectron lasers into vacuum and recording signals for each spatial and spectral channel pair. The stray light level is characterized by the pulse integral of the APD signals. Saturation of the signal occurs when the APD signal is clipped by the digitizer, which is equivalent to a pulse integral of 6000 mV ns; the noise level is 16 mV ns. The 1064 nm spectral channel collects the most stray light and has a saturated signal for all spatial channels. To bring the signal below the level of saturation, stacks of up to five neutral density filters (Hoya ND-25, OD 1 at 1064 nm) are inserted in the collection optics.

Note: Contributed paper, published as part of the Proceedings of the 21st Topical Conference on High-Temperature Plasma Diagnostics, Madison, Wisconsin, USA, June 2016.
[a)]Electronic mail: cjacobson@wisc.edu
[b)]Present address: Accuray Inc., Madison, Wisconsin 53717, USA.

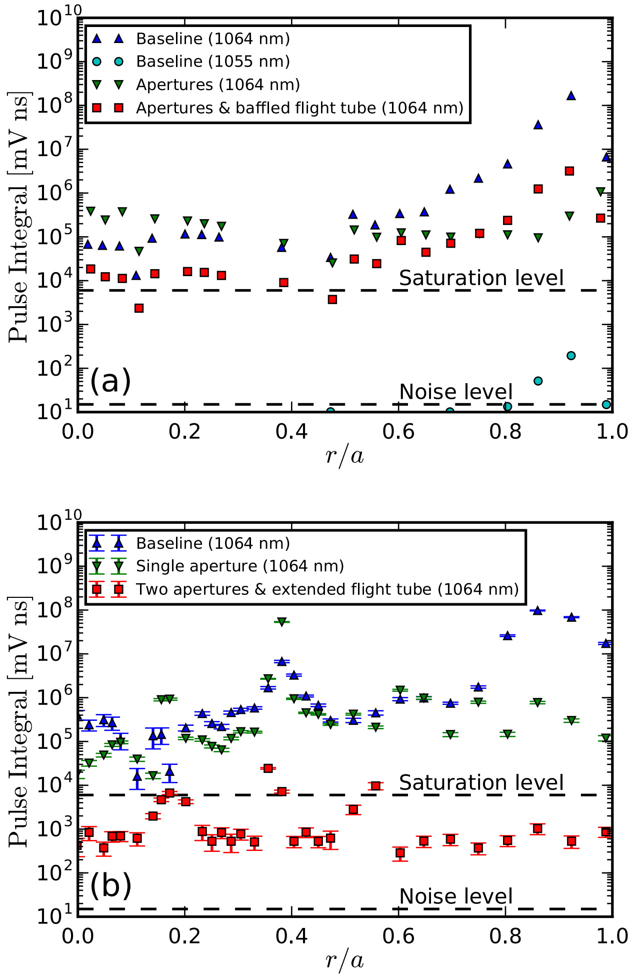

FIG. 1. (a) Measured and (b) simulated stray light levels. Saturation and noise levels are indicated by dashed lines. Uncertainty is determined from photon counting statistics.

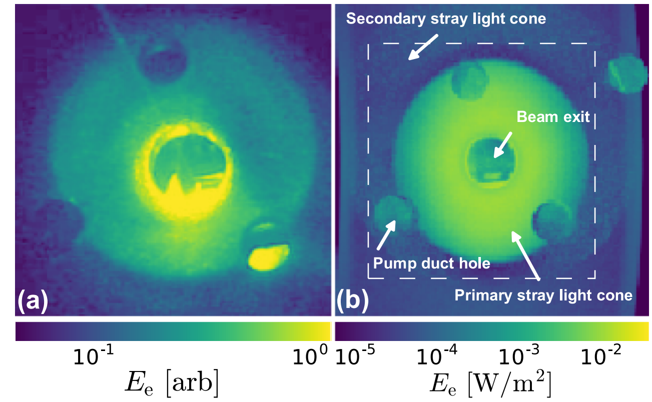

FIG. 2. Stray light surrounding the beam exit port at the bottom of the vacuum vessel (a) imaged by a modified webcam and (b) simulated by Zemax. The toroidal direction is vertical and the interior of MST is to the right. The dashed rectangle in (b) represents the approximate field of view in (a).

The signal level is corrected from its attenuated level for analysis. As shown in Fig. 1(a), baseline stray light levels are all above the saturation level in the 1064 nm channel. The large signal in the edge channels is an indication of stray light near the exit port, which is consistent with a diffuse stray light cone entering the plasma volume from the entrance port. Comparison of data taken with the MST vacuum vessel at vacuum versus atmospheric pressure determines that the dominant signal at atmospheric pressure is due to stray light and not Rayleigh or Raman scattering.

The adjacent spectral channel (centered at 1055 nm with 8 nm full width) records a significant signal for $r/a \geq 0.8$ due to a finite transmission of the filter out of band, which makes T_e measurements in those spatial channels impossible. To allow T_e measurements, the stray light levels in the 1064 nm channel should be less than $\sim 10^7$ mV ns.

A CCD-based webcam with the internal infrared filter removed is used to image stray light within the vacuum vessel, and while not calibrated, can provide a qualitative view of stray light sources. An image viewing the beam exit port is shown in Fig. 2(a). The image of a stray light cone is evident, along with stray light shining up through the exit port and pump duct holes. This suggests that adding properly sized apertures to reduce the size of the stray light cone to within the exit port and sealing pump duct holes near the laser exit port could vastly reduce stray light.

Black painted (Rust-Oleum 1916830) apertures ~10% larger than the beam diameter are placed at the entrance port and the alignment probe box output port. Additional apertures are placed at the input and output ports of a box enclosing the turning mirror and lens. As shown in Fig. 1(a), stray light levels are strongly reduced in the edge region, but are mostly unaffected in the core.

To characterize the effects of reflections within the entrance flight tube, the entrance flight tube is replaced by a polyvinyl chloride (PVC) pipe baffled with black foam (3M Velostat and Insul-Tube), with the apertures previously discussed still in place. Results are shown in Fig. 1(a). While these components are not vacuum-compatible, they demonstrate that stray light levels in the core-viewing channels can be reduced by using low reflectivity walls in the entrance flight tube. Note that slightly higher levels of stray light in the edge-viewing channels were observed, which could be due to the beam clipping foam within the flight tube.

For the case with apertures, the largest stray light signal of 10^6 mV ns is low enough to allow T_e measurements past $r/a \geq 0.75$ once implemented in a vacuum-compatible manner. However, overall stray light levels are insufficiently reduced to allow an absolute n_e calibration. Laser misalignment is found to be a contributor to stray light. When the laser is aligned to within 3 mm of the center of the vessel entrance port, stray light in the edge channels can be reduced by up to a factor of 30. Scatter from the Brewster windows and misaligned polarization of the lasers were not found to produce significant stray light levels.

III. OPTICAL MODELING

Optical modeling of stray light is performed using Zemax OpticStudio. The model is built of solid objects imported from a Solidworks model of MST using STEP format files. As shown in Fig. 3, the model is comprised of a 20° section

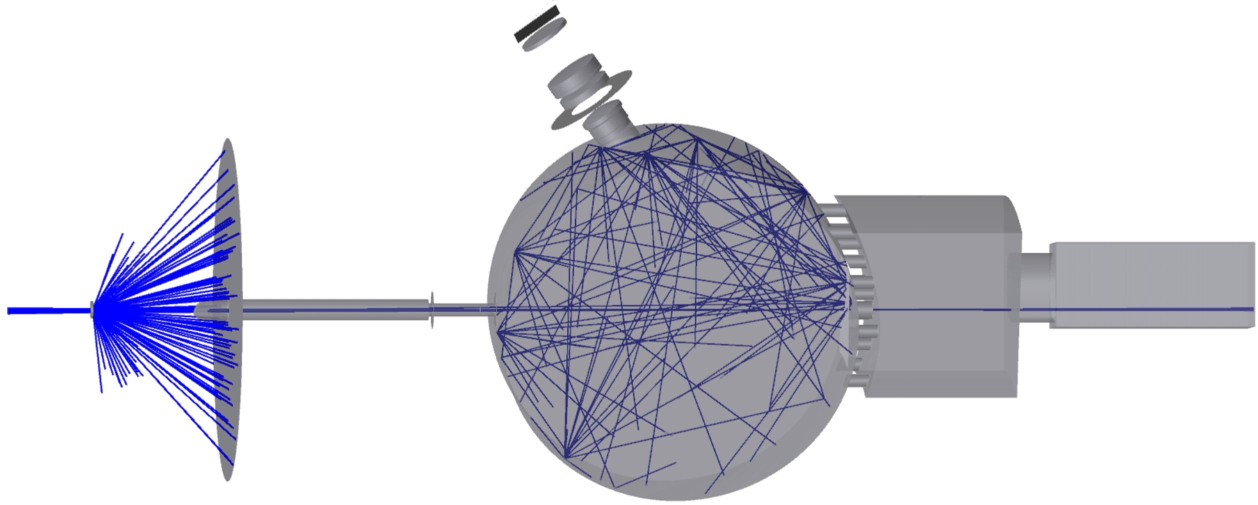

FIG. 3. An overview of the Zemax model in the baseline configuration. Modeled rays are shown in blue. An ideally absorbing plane stops rays from scattering directly from the focal lens to the viewing optics.

of the toroidal vacuum vessel and pump duct, the alignment probe box, entrance flight tube, and focal lens. Metallic faces are set to be aluminum with 10% Lambertian surface scatter, except for the vacuum vessel interior, which is set to 80%. Ideally absorbing faces are used to stop rays scattering outside of the toroidal section. The Brewster window is omitted from the model as the focal lens could become the vacuum interface. A diagnostic measures light incident on a plane above the bottom of the plasma volume. As shown in Fig. 2(b), the Zemax model qualitatively reproduces features observed by the modified webcam. A viewing optics model includes lenses along with fiber sizes, positions, and angles to act as a synthetic diagnostic to measure stray light for direct comparison with experimental measurements. Modeled normalized collected power P is scaled to the pulse integral $S = GN_iP\sigma$ where $G = 2.5 \times 10^{-1}$ mV ns is the APD gain factor and $N_i = 8 \times 10^{18}$ is the number of incident photons, assuming a laser energy of 1.5 J. The model focal lens scatter $\sigma = 1\%$ is tuned to match measured stray light levels. Fig. 1(b) shows that simulated baseline stray light profiles are similar in shape to experimental measurements. The increased level of stray light near $r/a = 0.4$ is attributed to stray light from the entrance port reflecting off the vessel wall and into the collection optics. Enlarging the entrance flight tube diameter from 63 mm to 150 mm and adding an aperture 6 cm above the entrance port (0.5 mm thick with a 3 mm gap around the beam) strongly reduce stray light in the edge, but reflections within the entrance flight tube result in little reduction elsewhere. Elongation of the entrance flight tube and the placement of two apertures, one at the entrance port and the other 0.82 m above, result in stray light low enough to allow T_e measurements at all radii and n_e at most radii. While this work is still in progress, candidate solutions will first be tested within the model before a final design is selected for implementation on the experiment. In order to most effectively mitigate stray light in other Thomson scattering diagnostics, the authors suggest performing both experimental measurements and numerical modeling.

SUPPLEMENTARY MATERIAL

See supplementary material for the digital format of the data shown in this paper.

ACKNOWLEDGMENTS

This material is based upon work supported by the U.S. Department of Energy, Office of Science, Office of Fusion Energy Sciences under Award No. DE-FC02-05ER54814.

[1]J. A. Reusch, M. T. Borchardt, D. J. Den Hartog, A. F. Falkowski, D. J. Holly, R. O'Connell, and H. D. Stephens, Rev. Sci. Instrum. **79**, 10E733 (2008).
[2]R. N. Dexter, D. W. Kerst, T. W. Lovell, and S. C. Prager, Fusion Technol. **19**, 131 (1991).
[3]C. J. Barth, M. N. A. Beurskens, C. C. Chu, A. J. H. Donné, N. J. Lopes Cardozo, J. Herranz, H. J. v. d. Meiden, and F. J. Pijper, Rev. Sci. Instrum. **68**, 3380 (1997).
[4]D. J. Schlossberg, M. W. Bongard, R. J. Fonck, N. L. Schoenbeck, and G. R. Winz, J. Instrum. **8**, C11019 (2013).
[5]J. P. Levesque, K. D. Litzner, M. E. Mauel, D. A. Maurer, G. A. Navratil, and T. S. Pedersen, Rev. Sci. Instrum. **82**, 033501 (2011).
[6]L. A. Berni and B. F. C. Albuquerque, Rev. Sci. Instrum. **81**, 123504 (2010).
[7]I. H. Hutchinson, *Principles of Plasma Diagnostics*, 2nd ed. (Cambridge University Press, 2002).